Acta Geochim (2019) 38(1):22–39
https://doi.org/10.1007/s11631-018-0268-5

ORIGINAL ARTICLE

Geochemistry and petrology of superpure quartzites from East Sayan Mountains, Russia

A. M. Fedorov[1,2,5] · V. A. Makrygina[1] · A. I. Nepomnyaschikh[1,4,5] · A. P. Zhaboedov[1,5] · A. V. Parshin[1,2,4] · V. F. Posokhov[3] · Yu. V. Sokolnikova[1,2]

Received: 5 July 2017 / Revised: 28 December 2017 / Accepted: 1 March 2018 / Published online: 8 March 2018

Abstract Quartzites are widespread within Earth's lithosphere, but their highly pure varieties occur quite infrequently. With the development of alternative energy sources, including solar, and with increasing demand for high-purity quartz for optics, interest has risen in high-purity silicon-bearing materials. The quartzites discovered in the southeast part of the Eastern Sayan Mountains are particularly attractive for exploration in terms of their raw material quality and feasibility to be enriched. For this reason, their genesis also merits study. Available geochemical data show that chemogenic ($d^{18}O > 29.2‰$) siliceous-carbonate sediments of the Irkut Formation are fairly pure (impurity elements < 800 ppm), and that half the impurities are easily removed carbonate components of the rock. Bedded quartzites remote from the intrusive granitoids and near-contact quartzites were recognized based on geochemical and petrographic data. Influenced by the Sumsunur granitoids, the near-contact quartzites originally contained $> 0.9\%$ impurities, but later, under the action of sliding slabs of ophiolite dynamothermal treatment reduced impurities to < 100 ppm, resulting in "superquartzites" (highly pure quartzites). The presence of only minor structural impurities is due to the enrichment capacity of superquartzites to 10.1 ppm (7.2 ppm under special conditions) of 10 elements: Fe, Al, Ti, Ca, Mg, Cu, Mn, Na, K, and Li.

✉ A. M. Fedorov
sashaf@igc.irk.ru

[1] A.P.Vinogradov Institute of Geochemistry SB RAS, Irkutsk, Russia 664033

[2] Irkutsk National Research Technical University, Irkutsk, Russia 664074

[3] Geological Institute SB RAS, Ulan-Ude, Russia 670047

[4] Irkutsk State University, Irkutsk, Russia 664003

[5] Irkutsk Scientific Center SB RAS, Irkutsk, Russia 664033

Graphical Abstract

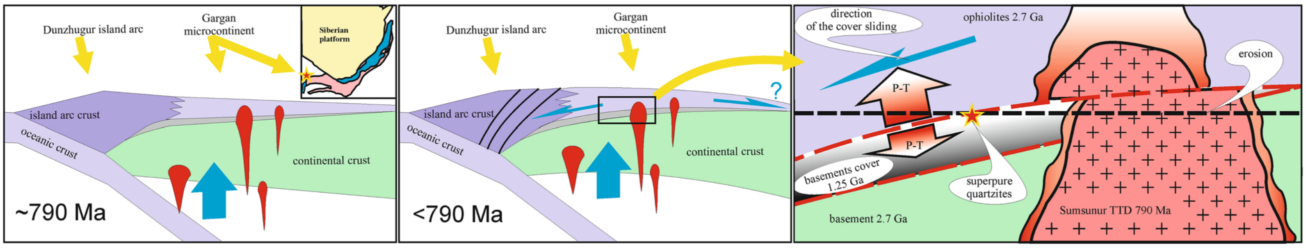

Keywords High-purity quartz · Superquartzite · Gravitational sliding · Dynamic metamorphism · Recrystallization

1 Introduction

Beginning in the mid-1960s, in the industrially developed countries of Europe, the USA, and Japan, fragments of crystalline quartz obtained through enrichment of rock crystal have been used to produce one-component quartz glass (Jung 1992). Geological and technological work performed by Unimin Corporation in the USA on the profound chemical purification of quartz and quartz-muscovite plagiomigmatites paragenetically associated with leucocratic pegmatoid muscovite granites resulted in production of high-purity concentrates corresponding to the Iota standard (Krylova et al. 2003), and requirements of the feedstock used for melting of one-component transparent quartz glass were established (Krylova et al. 2003, 2004; Bydtaeva et al. 2006a, b; Gotze 2012).

Russia is one of few countries where high-purity quartz is widely employed in industry, and special efforts have been undertaken to develop the mineral base of chemically pure quartz materials (Serykh et al. 2003; Danilevskaya et al. 2004; Kuznetsov et al. 2005; Danilevskaya and Schiptsov 2007). High-purity quartz has various applications, including solar power engineering (Nepomnyashchikh et al. 2000) and optic quartz glass production (Nepomnyashchikh et al. 2017). As noted above, Unimin developed specific technologies to profoundly enrich quartz glass of ordinary quality to one-component quartz glass (Krylova et al. 2003). Additionally, superquartzites can be enriched in pulsation columns (Vorob'ev et al. 2003) from non-structural impurities to derive high-quality groats (Krylova et al. 2004). These technologies demonstrate huge potential for quartzites. Compared to vein quartz deposits, quartzite reserves are more abundant and more suitable for mining.

Although quartzites are fairly widespread in Earth's lithosphere among sedimentary-metamorphic rocks, the highly-pure varieties (impurity content less than 0.1%) are quite rare (Vorob'ev et al. 2003; Muller et al. 2007; Gotze 2012). Within the Sayan-Baikal-Patom belt, in addition to the sole developed Cheremshanka deposit (Tsarev et al. 2007), deposits and occurrences of quartzites and micro-quartzites have been discovered in the Western Baikal region (Petrova et al. 1996; Makrygina and Fedorov 2013) and East Sayan Mountains. It is noteworthy that highly pure quartzite mostly occurs in the Bural-Sardyk deposit in the southeast of the East Sayan Mountains (Vorob'ev et al. 2003; Fedorov et al. 2012), making it the site of major prospected and evaluated reserves.

Hypotheses related to the formation of superpure quartzites have been described in numerous publications (Vorob'ev et al. 2003; Bydtaeva et al. 2006b; Fedorov et al. 2012; Makrygina and Fedorov 2013; Kabanova et al. 2014; Anfilogov et al. 2015).

In the view of Vorob'ev et al. (2003), the protolith of quartz consists of chemogenous-sedimentary siliceous-carbonate sequences with minor impurities of coaly substance and terrigenous material regionally metamorphosed under greenschist facies. The authors believe that granitoid intrusion of the Sumsunur complex caused metasomatic alterations including loss of impurity components, leading to recrystallization of the quartz substratum with a sharp increase of grain size and eventual formation of subvertical bodies of superquartzites in the apical parts of folds.

Some authors (Bydtaeva et al. 2006b) assume that transformation of initial siliceous rocks took place in shear structures under effect of carbonic dioxide aqueous fluid (more pure than magmatogenic) generated during tectonic-metasomatic transformation of limestones. However, the observed subhorizontal morphology of productive bodies excludes subvertical blowout and consequently purification of quartzites, both in the first and second cases.

Around the same time, when prospecting the deposit, V. P. Tabinaev and S. D. Tsutsar (oral comm., not published)

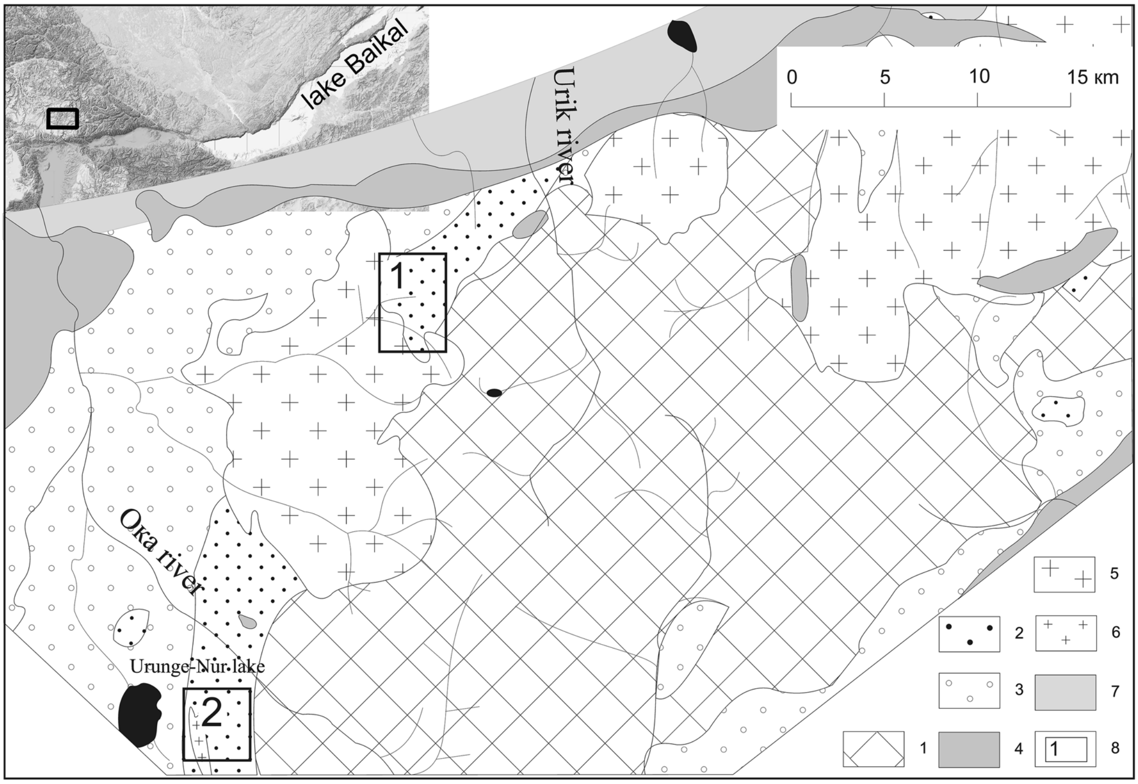

Fig. 1 Northern part of Tuva-Mongolian Massif. 1. Basement of the Gargan Block (Archean-Lower Proterozoic); 2. fields of discolored quartzites within Irkut Formation; 3. Gargan Block cover (Irkut Formation), Middle-Upper Riphean; 4. Upper Riphean ophiolite complex; 5. granitoids of the Sumsunur rock assemblages, Upper Riphean; 6. granitoids of the Holba rock assemblage; 7. Tuva-Mongolian Massif cover, Upper Riphean; 8. borders of survey sites numbered as 1: Bural-Sardyk deposit and 2: Urunge-Nur occurrence

observed a subhorizonal bedded formation of productive bodies, leading them to conclude that metasomatic alterations of coastal-marine quartz sandstones proceeded under the heat field of granitoid intrusion of the Sumsunur complex. This can be compared with the effect of smoothing iron over wet cloth.

From the perspective of petrographic and mineralogic studies, some authors (Kabanova et al. 2014; Anfilogov et al. 2015) have proposed a model of the quartzite formaton at Bural-Sardyk as being due to hydrothermal transformation of coaly quartzites of the Irkut Formation along subvertical tectonic dislocations. Because this scheme disregards the results of prospecting and a previous survey, we support the first hypothesis discussed—that of Vorob'ev et al. (2003).

A new model has been discussed since 2011 (Fedorov et al. 2012; Makrygina and Fedorov 2013). It implies dynamic metamorphism or dynamic metasomatism transformation of pure initial quartzites under the action of ophiolite cover slabs overthrusting due to obduction or sliding due to uplifting of the Gargan Block center.

Because opinions on the origin of highly pure quartzites vary, and at times are mutually exclusive, thorough study is needed of formation conditions with modern methods and instruments, e.g. inductively coupled plasma mass spectrometry (ICP-MS) and isotope geochemistry. Neighboring areas should be surveyed as well to compare and reconstruct the geodynamic setting where deposits formed. In this paper, we discuss the model of highly pure quartzite formation in the East Sayan Mountains by dynamic-thermal treatment of primary rocks through the action of sliding slabs of ophiolite cover and their autolys from the zone of detachment to adjacent bedded formations.

2 Geologic features

2.1 Regional geology and tectonic position

The survey area is located about 200 km west of the southern Baikal termination within the Siberian Platform foldbelt (Fig. 1). The Bural-Sardyk deposit lies in the west of the Gargan Block. Its basement outcrops in the east of the well-studied Tuva-Mongolian microcontinent adjoining the Siberian Craton along the Major Sayan Fault (Sklyarov and Dobretsov 1987; Kuzmichev 2001, 2004; Kuzmichev et al. 2001; Belichenko et al. 2003; Gordienko 2006; Reznitsky et al. 2007; Zorin et al. 2009; Demonterova et al. 2011; Safonova and Santosh 2014). The Gargan Block basement, its metamorphism dated by U–Pb as 2.7 Ga (Anisimova et al. 2009), is composed of gneisses, plagiomigmatites, tonalite-gneisses, and amphibolites. The amphibolitic degree of rock metamorphism predominates, but in places it reaches the granulite facies (Kuzmichev 2004.).

The basement of the block is overlapped by a sedimentary chemogenous-volcanogenic cover. Its lower bedded sequence of superpure quartzites is composed of the Riphean shale-carbonate-quartzite formations of the Irkut Formation, widespread in the northern and north-western termination of the block core. The basal horizon of the Irkut Formation is composed of quartzite-sandstones with regenerative quartz and sericite cement, quartz siltstones, and sericite-quartz shales. They are overlapped by limestones and dolomites with stromatolites and thin strata of black quartz-sericite shales containing talc, graphite, and manganocummingtonite. The uppermost part of the Bural-Sardyk deposit is composed of the quartzites discussed in this study. At the bottom, quartzites are black and dark grey, gradually lightening upwards into grey and white; superquartzites complete the cross-section. The total thickness of siliceous-carbonate sediments of the Irkut Formation at this site reaches 800–1200 m. It terminates west of the Bural-Sardyk deposit with overlapping quartzites alternated with limestones and dolomites (Semeikin et al. 2006).

The Irkut's age is estimated as 1.25 Ga from Sr-chemostratigraphic data acquired from carbonates (Kuznetsov et al. 2010). The folded deformation of silica-carbonaceous sediments of the Gargan Block and subsequent obduction of oceanic crust set conditions for greenschist metamorphism. In this work we discuss quartzites of two units: (1) Urunge-Nur occurrence of poorly metamorphosed quartzites and (2) Bural-Sardyk deposit of well-preserved highly pure quartzites.

The slabs of the Upper Riphean ophiolites, currently framing the Gargan Block in the west, north-west, and south-east are fragments of deformed and eroded allochthon, which possibly overlapped its larger part (Dobretsov 1985; Sklyarov and Dobretsov 1987; Kuzmichev 2004). In the west, ophiolites make up three major sliced sheets.

The intrusions of the Sumsunur rock assemblage of tonalite-trondjemite-dacite series plagiogranites have been dated by the U–Pb method as 790 Ma (Kuzmichev 2004). The south of the Bural-Sardyk deposit hosts post-batholith dykes, sills, and stocks composed of microdiorites, gabbro-porphyrites, and diorite porphyrites, as well as rhyolites and dacites (Grebenshchikova and Koval 2004). In the south, the Gargan Block is crosscut by Early Paleozoic granitoids of the Munku-Sardyk Range, which have been U–Pb dated at 481 ± 2 Ma (Reznitsky et al. 2007).

Within the study area, both recent and inherited tectonic dislocations have been recognized: e.g. faults, shifts, and slickensides directed from the center toward the periphery of the block.

2.2 Geologic structure of Bural-Sardyk deposit

The Bural-Sardyk deposit is dominated by northeast-extending ranges and hills, the Bural-Sardyk Mount being the main peak at 2788 m. In the apical parts of this massif, some exposures of discolored quartzite of the Bural-Sardyk deposit crop out at the surface (Fig. 2).

Quartzites constitute the most widespread group of rocks. While prospecting, drilling penetrated productive bodies of superquartzites and bedded quartzites sloping gently at 4°–5° towards WNW.

Two cross-section types have defined by composition of impurities and structure: (1) at significant distance from and (2) near the contact of Sumsunur granitoids (Fig. 4). In both cases black and dark-grey carbonaceous quartzites occur in the basement, gradually lightening upward into discolored (light-grey and white) quartzites with bed thickness of tens of meters. The purest quartzites—superquartzites—sit at the cross-section top. Their thickness varies from 6 to 12 m. The near-contact quartzites some tens of meters away from the contact with granites contain the impurities of sericite, chlorite, and a few grains of ore minerals (Figs. 4, 1b–4b). Grain size and degree of crystallization increase upward.

2.3 Geologic structure of the Urunge-Nur occurrence

The Urunge-Nur primarily consists of Quaternary glacial sediments overlying the extensive mid-mountainous plateau (Fig. 1). The left Oka riverside exposes the rocks of the Irkut Formation. These are white and grey carbonate-

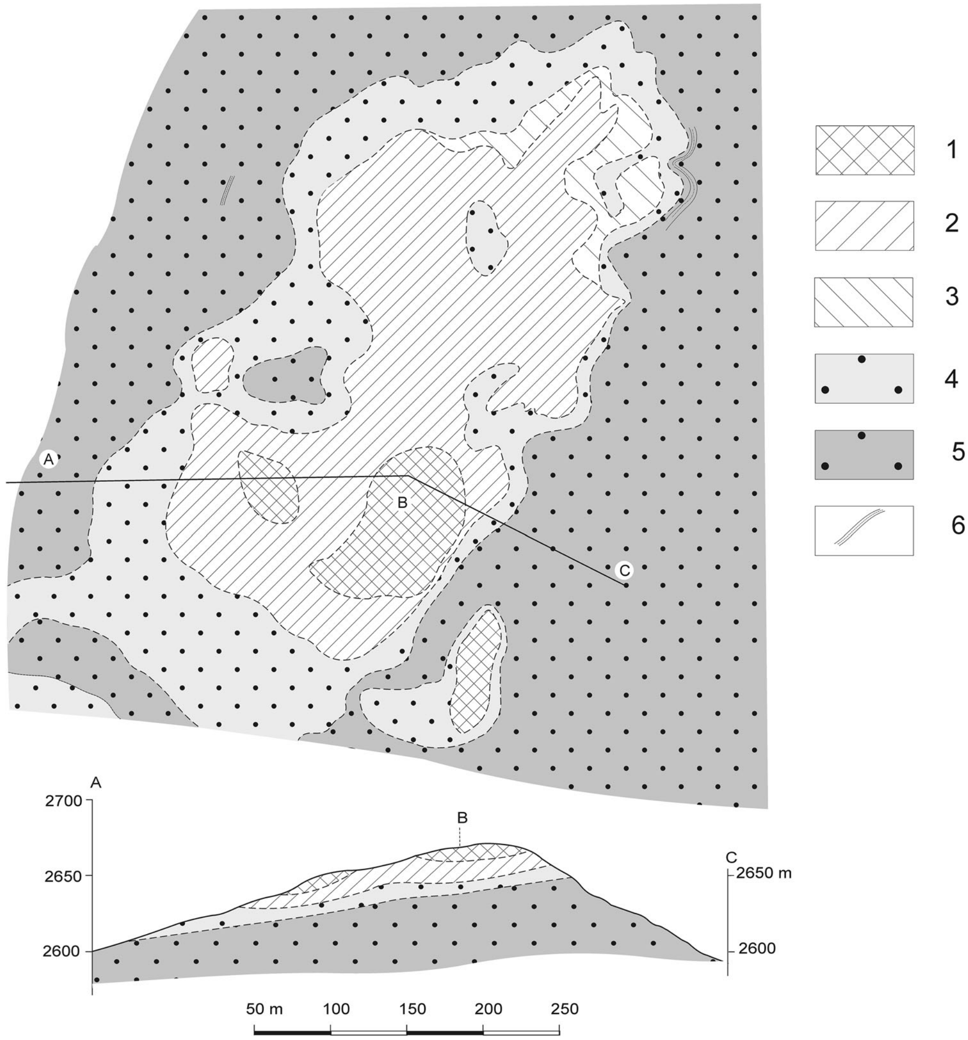

Fig. 2 Geology of Bural-Sardyk deposit. 1. superquartzites; 2. white fine-grained quartzites; 3. sandy quartzites being the products of weathering of dynamic-metamorphic quartzite formations; 4. grey and light-grey microquartzites; 5. black, stone-like micro quartzites; 6. carbonaceous-clayey schists

siliceous banded rocks of pinkish and brownish shades—intercalated micrograin source quartzites, e.g. silicite and limestone. The visible part of sediments represents the stratum dipping 5°–10° toward NW 320°–340°. It is split by a system of subvertical rupture dislocations of varying extent. They are responsible for low-amplitude undulation of beds and, accordingly, for the scatter of observed azimuths and angles of incidence. Thickness of quartzite streaks is from a few millimeters to centimeters, and in places up to 0.5 m. In these rocks the thickness of silicite beds is generally larger than carbonate ones, and the quartz/carbonate component ratio is considerable.

The true thickness of the outcrop of siliceous-carbonate beds is estimated as 200 m. In the west they are gradually replaced by carbonate rocks (grey and dark-grey limestones), which are cross cut by the intrusive bodies of the Kholba and Munku-Sardyk rock assemblages of the Paleozoic age.

Even if the rocks of the Irkut Formation experienced decoloration and recrystallization, a close thin alternation of quartzites with limestones and fairly uniform appearance suggest that aside from regional greenschist facies metamorphism, they have not undergone superimposed metamorphism. That is why the productive bodies of dynamometamorphic quartzites are revealed on this very site (Fig. 3).

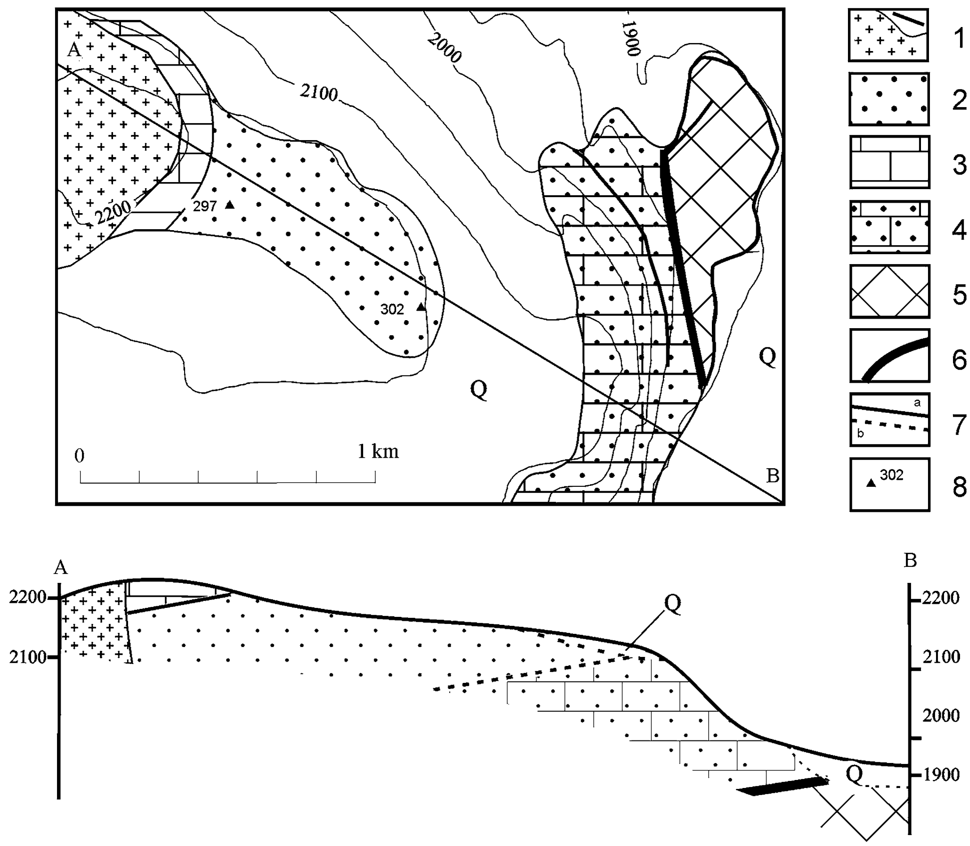

Fig. 3 Geological scheme of the Urunge-Nur site. 1. Quaternary sediments; 2. dykes and sills of granitoids of the Kholba rock assemblage; 3. grey and dark-grey fine-grained quartzites; 4. siliceous-carbonate rocks; 5. Early Proterozoic crystalline rocks of the Gargan block basement; 6. shear dislocations; 7. elements of occurrence; 8. line of geochemical profile

3 Methodology

Although the composition of quartzites seems simple, appropriate analysis of economic quartz ore has become feasible only with high-precision and sensitive ICP-MS methods. To avoid contamination, sample preparation protocol must be carefully followed.

Preparing samples of highly pure quartz to be analyzed by ICP-MS includes: (a) flushing the specimen in distilled water; (b) chemical purification of quartz pieces of − 5 + 20 mm fraction from sorbed components on the surface in 10% solution of super clean hydrochloric acid (HCl); (c) thermal crushing via heating to T = 900 °C and cooling by deionized water; and (d) grinding to 0.1–0.5 mm in a mortar with a pestle made of superquartzite recovered in the Bural-Sardyk deposit (to avoid contamination of material with the device substance).

Produced quartz concentrates were analyzed at the Institute of Geochemistry (SB RAS): e.g. ICP-MS (Nepomnyashchikh et al. 2017), atomic emission spectrometry (AES), and flame photometry (FP). To determine element contents, a high-resolution ICP-MS ELEMENT-2 (Finnigan MAT, Germany) was used. The FP method was used to determine alkaline elements. The flame photometer with a propane-air flame was combined with a DFS-12 (LOMO, Russia) spectrometer.

The accuracy of determinations was estimated by analyzing high-purity quartz concentrates of IOTA grade or by applying the standard addition method.

For determination of main elements with Direct AES, multichannel spectra recording was fulfilled by spectral installation, including a diffraction spectrograph DFS-458 C (PO KOMZ, Russia) and multichannel analyzer of emission spectra MAES (VMK-Optoelektronika, Russia) based on a microassembly of eight photodiodes. The generator “Vesuvius” (VMK-Optoelektronika, Russia) of direct/alternate current was utilized as the spectra excitation source. On/off switching is synchronous with MAES.

The isotope composition of oxygen as O_2 was defined by gas mass-spectrometer FINNIGAN MAT 253 with utilization of a double system of inflow in classic variant (reference sample). To determine $\delta^{18}O$ values, samples were prepared by lazer fluorination (LF) in the presence of BrF_5 reagent. The array involves the device MIR 10-30 heating system, including laser CO_2 with capacity 100 Wt and wavelength 10.6 μm in the infrared area, which allows heating of analyzed minerals to 1000 °C. It also contains the vacuum line for purifying the released gas with cryogenic traps and with special sorbent cooled by liquid nitrogen for final concentration of oxygen.

The proceeding reaction was visually monitored to observe completeness of decomposition. At times we had

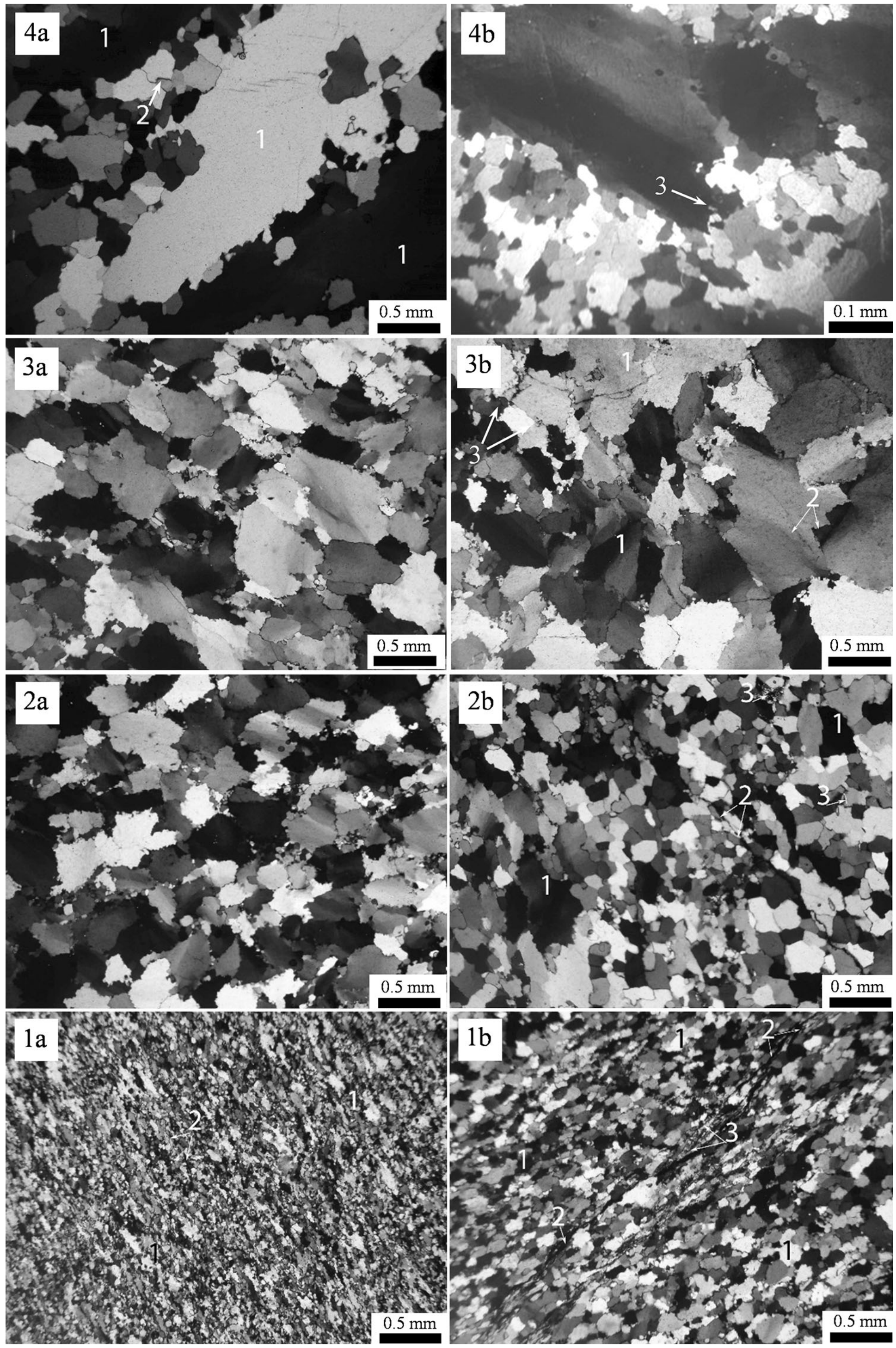

Fig. 4 Main varieties of quartzites of Bural-Sardyk deposit (thin sections): **a**. cross-section from top to bottom far from the contact with granitoids; **b**. the same but close to the contact with granitoids. 1–4. increase of recrystallization degree before superquartzites (4). Thin section images: 1. quartz, 2. graphite, 3. sericite. Crossed polarizers

to change the regime (output and focusing of laser beam) to achieve complete sample combustion. In LF, oxygen is not fractionated because of minor time for reaction and high temperatutre. Decomposition of one sample requires about 15–20 min, minimizing contamination of obtained gas by atmospheric impurities.

The fragments of only pure minerals weighing 1.5–2.5 mg were used for isotope analysis. The $\delta^{18}O$ values were calculated versus international standard NBS-28 (quartz) and checked with internal standard GI-1 (quartz) and one Polaris (quartz) of IGEM RAS. The error of estimated $\delta^{18}O$ values was (1 s) $\pm$ 0.2‰.

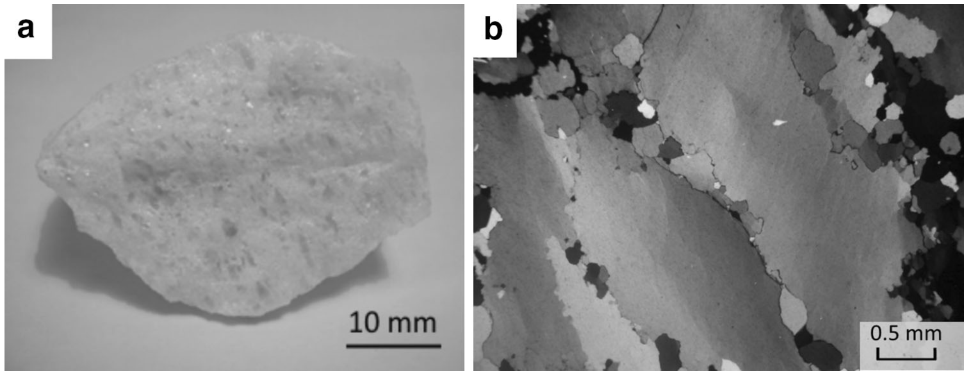

Fig. 5 Superquartzite sample: white monomineral rock of porphyry-like structure. a on the back ground of fine-grained basic mass there are subparallel oriented transparent quartz grains, their size over the long axis varying from 1 to 4 mm. b the interstices contain grains of the same shape with size varying from 0.8 × 0.6 to 1.2 × 0.4 mm (30%) and finest isometric grains from 0.05 to 0.3 mm across (20%). The structure is porphyry-like. Polarizers: a –//, b–+

The petrographic study of quartzites of the Bural-Sardyk deposit was performed in polarized light with an Olympus BX-51 microscope equipped with photo camera Olympus C-4000 and microscope-binocular MPSU-1 having a wide field of vision.

4 Results

4.1 Petrography of quartzites

The petrographic study of quartzite was intended to: (1) identify grain size and genetic origin; (2) acquire granulometric characteristics for technological processing. As stated before, two basic types of cross-section are recognized by relationship with granitoids at the Bural-Sardyk deposit. In our study, we considered cross-sections as representative or reference for a particular geological setting. The Urunge-Nur quartzites represent initial rocks for formation of the other types of quartzites; some near-contact alteration exists (Fig. 4).

Some petrographic varieties of quartzites have been recognized by grain size, structure, texture, and color: siliceous micro quartzites of bedded and lense-like bodies, from black and dark-grey to lighter ones with banded texture up to the white color; and from microquartzites to medium-grained and porphyry-like superquartzites.

4.1.1 Petrographic features of quartzites at Bural-Sardyk deposit

4.1.1.1 First type of cross-section: bedded bodies (Figs. 4, 1a–4a) Carbon-bearing sedimentary-metamorphic silica-like microquartzites, dark-grey to black, occur as bedded and lens-like bodies at the cross-section bottom and are host rocks for productive bodies (Figs. 4, 1a). These microquartzites are quite similar to the black (dark-grey) siliceous separations in dolomites occurring beyond the deposit. They are distinguished by their voluminous spread and larger grain size. At the surveyed site of the Irkut Formation outcrop, their masses are comparable with carbonate (dolomite) substratum, and within the deposit they predominate over the latter.

Carbon-bearing microquartzites include elongated grains with notched boundaries over the long axis, predominantly sized 0.1–0.2 mm and smaller, making up 98%–99% of the rock (Figs. 4, 1a). The particles of finely-dispersed carbonaceous substance (0.5%–2%) fill the interstices between quartz grains, in places producing hair-like streaks. The structure is microgranoblastic, notched; the texture is poorly banded because of the irregular distribution of particles of carbonaceous substance.

In some sites these rocks contain the relics of ultra-micrograined (particle size about 0.004 mm) quartz rocks, pigmented by finely-dispersed carbonaceous material. These ultramicroquartzites represent early relict forms of lithified siliceous sediment observed both in the productive bedded sequence and in the siliceous dolomites within the deposit environment. This is the evidence for their belonging to the same early generation.

Upsection quartzites are discolored, with increasing quartz grain size; quartzites lack impurities, primarily carbonaceous substance, causing the color to whiten upward (Figs. 4, 1a–33a). The discolored quartzites represent the main economic mineralization for volume and quality. The boundaries between quartzites of different types are diffused; alterations proceed gradually. Diversity of textures of light colored quartzites is remarkable: banded, spotted-striped, netted, or breccia-like due to the fracturing and bedding pattern. The microquartzites closest to the primary sediments have elongated grains parallel to bedding; the discolored—and particularly

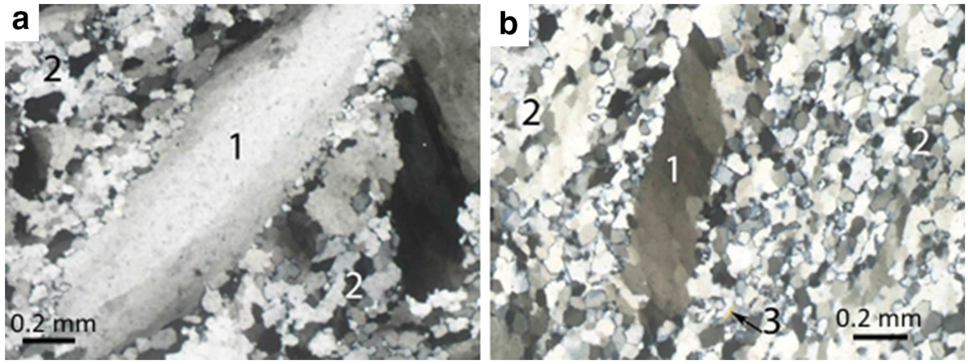

Fig. 6 Initial quartzite is white; displays thin grey stripes formed with carbonaceous substance, carbonate, and sericite. 1. medium elongated grains of quartz with notched margins and wavy extinction, 2. micro grained quartz, 3. sericite scale. **a**. at distance from the contact with granitoids, **b**. in the near-contact zone. Nicols +

superquartzites—display well-expressed orientation linked with dynamic movement of rock masses (Figs. 4, 4a).

Superquartzites enclosed in the upper cross-section are characterized by practically monomineral quartz composition and coarsely irregular porphyry-like structure (Fig. 5). In places, superquartzites occur as thin (few cm) seams or lenses amongst white, fine-grained quartzites. Coarse grains sized from 1.6×0.5 to $4 \times 2\ mm^2$, and rarely to $9.4 \times 6.4\ mm^2$, constitute 5%–50% or more of the volume. These grains are irregularly shaped, often elongated, and their boundaries are winding and notched. They feature subparallel orientation of large and transparent quartz grains (Figs. 4, 4a, 5a, b). The elongated grains of medium size varying from 0.5×0.3 to $1.4 \times 0.6\ mm^2$ display notched outlines; over the long axis they are oriented identically to the large grains. Large- and medium-sized grains are surrounded by smaller isometrically shaped grains from 0.03 to 0.3 mm, in places forming micro-fine-grained aggregate with granoblastic mosaic structure. Superquartzites contain fine fluid inclusions of flattened isometric and rounded shapes. They produce narrow chains and bands. Sodium is the principal component of fluid inclusions, whereas K and Mg are observed at background level (Volkova et al. 2017).

Such structure indicates superquartzite formation through recrystallization with grain coarsening under dynamic stress (Grigoriev 1956; Popov 2011).

4.1.1.2 Second type of cross-section: near-contact quartzites (Figs. 4, 1b–4b) This cross-section begins with dark micrograined quartzites gradually getting coarser and eventually becoming superquartzites. Near the contact with granites, these rocks include more impurities of sericite, chlorite, and ore minerals commonly located in the interstices. Thus, the near-contact quartzites are distinguished by plentiful impurities of mica due to the impact of granites. Upsection, quartz grain size increases, whereas the amount of extraneous impurities and carbonaceous substance decreases (Figs. 4, 1b–4b). This is evidence for the metamorphic purification process being later than the effect of granites.

4.1.2 Petrographic features of quartzites of Urunge-Nur occurrence

Initial quartzites of the Urunge-Nur site represent quartz rocks split into characteristic schistose blocks by thin quartz veinlets and white-to-cream carbonate streaks. Their color varies from purely white to dark-grey with diverse transitional hues due to irregularly distributed coaly substance. Within leached carbonate interbeds they exhibit sublayered caverns.

Initial quartzites petrographically represent micrograined (grain size generally < 0.01 mm) monomineral quartz rocks bearing a minor amount of carbonate and thin sericite scales. In thin-section, the quartzite bulk is composed of slightly elongated (95%–97%) and isometric (3%–5%) ultra-micro grains with even- or cloudy-, and in some cases cloudy-mosaic, decay. Nearly all slightly elongated grains of basic mass are oriented in the same direction and display wavy-notched and fairly distinct margins. Fine (0.1 mm) quartz grains occur either sporadically as isometric nodules in the bulk mass, or within cracks and streaks. Greatly elongated quartz grains lying along cracks; they have cloudy-mosaic or cloudy-wavy extinction, and in half the cases display distinct notched-wavy margins.

In initial quartzites, mineral impurities (mostly calcite and sericite) are generally found within systems of cracks. Large cracks (up to 0.1 mm) are commonly healed with calcite and quartz. Calcite observed within cracks occurs as the dotted line of elongated or massive crystal. In rare cases there are well-faceted rhomb-like crystals. The remaining cracks are healed with quartz. Cericite is observed through the system of subparallel, isolated S-like detachment cracks or strike-slip faults of varying size, and it predominates in the near-contact zone. The cracks are mostly about 0.1 mm, and in rare cases up to 1 mm (Fig. 6).

Table 1 Composition of major components in quartz varieties of Irkut Formation (East Sayan Mountains) (ppm)

Element	Initial quartzite, Urunge-Nur	Black quartzite, Bural-Sar'dag	Light grey quartzite, Bural-Sar'dag	Superquartzite, Bural-Sar'dag	Initial quartzite, Urunge-Nur	Dark-grey quartzite, Bural-Sar'dag
					Near-contact rocks	
	Analytical method (number of investigated samples)					
	ICP-MS (4)	AES (11)	AES (39)	ICP-MS (8)	ICP-MS (4)	ICP-MS (3)
	The content of elements (ppm)					
Al	*41*	70	107	33	*649*	5779
	20–68	20–257	9–475	9–59	*216–1289*	3488–8773
Ti	*1.2*	13.6	16.2	4.1	*20*	342
	0.9–1.5	1.3–113	0.1–252	0.4–23	*9.5–30*	104–612
Fe	*24.6*	100	97.8	9.2	*46*	596
	9.9–48	17–500	5–887	4.8–23	*15–94*	302–876
Mn	*1.6*	0.54	1.1	0.05	*2.0*	2.4
	0.8–2.7	0.1–1	0.1–21	0.02–0.11	*0.1–4.6*	0.7–4.5
Mg	*226*	40.6	59.2	1.7	*722*	239
	45–505	3–170	3–740	0.5–2.7	*83–1668*	185–278
Ca	*455*	8.6	15.7	2.5	*1374*	144
	93–1049	5–20	5–60	1.5–3.8	*4–3437*	24–217
Na	*5.0*	12.3*	10.2*	5.0	*11.0*	227
	4–7	6–26	3–40	3.5–7.9	*6.4–16*	60–321
K	*11.0*	157*	85.5*	6.1	*243*	2033
	5–16	47–311	7–100	1.4–11	*83–452*	1228–3090
P	*0.60*	4**	3.9***	0.69	*4.0*	76.3
	0.5–0.8	1–9	2–13	0.5–0.9	*2.4–7.4*	17–110
B	*0.16*	2.02	2.4	0.17	*1.0*	20.7
	0.04–0.3	0.5–4	0.5–7.1	0.12–0.26	*0.4–1.7*	15–28
Total	*766*	430	381	62.5	*3072*	9459

Determinations are performed at Institute of Geochemistry SB RAS (Irkutsk, Russia) with ICP-MS (by Sokolnikova Yu.V., Ponomareva V.Yu.), AES (by Vasilyeva I.E.) and FP* (by Sokolnikova Yu.V.)

**Labeled the results were obtained for 6 samples and ***labeled the results were obtained for 24 samples

4.2 Geochemistry of quartzites

4.2.1 Major and rare elements in quartzites of the East Sayan Mountains

At this deposit, practically all quartzite varieties are fairly pure relative to medium quartzite sandstones of the Cheremshanka deposit in the Republic of Buryatia referred to as the elite type for quality of raw material used for silicon production at JSC Kremniy in Shelikhov town (Irkutsk Region). They contain 2500–3000 ppm summary impurities (Fe + Al + Ca)—tenfold that found in the discolored varieties and 5-to-8-fold that in black quartzites at Bural-Sardyk (Tables 1, 2) (Tsarev et al. 2007).

In previous work (Makrygina and Fedorov 2013), we have discussed low major and trace element contents in the cross-sections remote from granitoids and elevated levels in the near-contact varieties (Table 2).

Black and dark-grey quartzites of bedded bodies closest to the original ones show high dispersion of impurity contents. Vorob'ev et al. (2003) linked this to irregular lit-par-lit distribution of terrigenous impurity in the initial siliceous sediments. The authors point out that the enhanced dispersion of impurity component contents is inherited due to their irregular distribution in the substratum.

The light-grey and grey quartzites show a fairly broad scatter of values of element-impurity varying from 40.9 to 500 ppm and more. In four out of 42 samples, the content of the sum of petrogenic elements is less than 100 ppm; in eight samples from 100 to 200 ppm; in fourteen samples from 200 to 300 ppm; and in the remainder, over 300 ppm. The mean content of the sum of petrogenic elements in 42 samples reaches 379 ppm (Table 1).

Table 2 Mean contents of impurity elements in the main quartz varieties

Element	Initial quartzite, Urunge-Nur	Black quartzite, Bural-Sar'dag	Light grey quartzite Bural-Sar'dag	Superquartzite, Bural-Sar'dag	Initial quartzite Urunge-Nur Near-contact rocks	Dark-grey quartzite Bural-Sar'dag
	Analytical method (number of investigated samples)					
	ICP-MS (4)	AES (11)	AES (39)	ICP-MS (8)	ICP-MS (4)	ICP-MS (3)
	The content of impurities (ppm)					
Rb	*0.046*	–	–	0.031	*0.88*	7.1
	0.01–0.09			0.009–0.056	*0.35–1.74*	4.8–9.5
Ba	*0.67*	–	–	0.61	*13.5*	54.0
	0.43–1.16			0.22–1.2	*5.2–17.2*	29–82
Sr	*0.44*	–	–	0.14	*2.4*	4.8
	0.24–0.87			0.07–0.33	*0.17–2.8*	2–6.6
Nb	*0.014*	–	–	0.017	*0.11*	1.6
	0.006–0.02			0.002–0.028	*0.05–0.2*	0.6–2.4
Zr	*0.16*	1.11	1.04*	0.26	*0.76*	6.7
	0.09–0.24	0.3–5	0.5–4	0.02–0.52	*0.4–1.34*	2.3–9.8
U	*0.13*	–	–	0.18	*0.078*	0.21
	0.02–0.42			0.019–0.36	*0.04–0.14*	0.11–0.26
Th	*0.013*	–	–	0.006	*0.078*	0.44
	0.006–0.03			0.001–0.01	*0.02–0.13*	0.22–0.57
Mo	*0.004*	–	–	0.025	*0.003*	0.019
	0.003–0.007			0.005–0.02	*0.003–0.004*	0.005–0.04
Pb	*0.091*	0.6**	0.5***	0.033	*0.10*	0.23
	0.02–1.3	0.3–0.9	0.01–1.3	0.02–0.06	*0.07–0.15*	0.21–0.27
Zn	*0.69*	5**	4.3***	0.19	*0.47*	2.2
	0.25–1.12		2–5	0.1–0.3	*0.2–0.77*	1.3–3.2
Sn	*0.111*	–	–	0.095	*0.094*	0.20
	0.004–0.2			0.01–0.47	*0.04–0.22*	0.11–0.26
Cu	*0.53*	1	0.93	0.80	*0.96*	1.67
	0.4–0.7	0.5–2.3	0.3–2.8	0.31–1.3	*0.7–1.3*	0.8–2.8
Co	*0.007*	1**	0.73***	0.004	*0.012*	0.15
	0.004–0.014	0.7–1.5	0.7–1.5	0.002–0.005	*0.004–0.02*	0.05–0.22
Ni	*0.084*	0.38	0.48	0.30	*0.074*	0.81
	0.02–0.2	0.2–0.7	0.2–1.2	0.1–0.3	*0.005–0.17*	0.34–1.2
Cr	*0.27*	5.15	5.38	0.074	*0.67*	10.0
	0.12–0.5	0.5–9.3	0.5–18	0.01–0.1	*0.3–1.4*	4.3–15
V	*0.23*	1.1	0.9	0.14	*1.29*	49.3
	0.09–0.34	0.5–4.6	0.5–1.5	0.01–0.2	*0.6–1.5*	25–71
Ge	*1.5*	–	–	1.4	*2.2*	1.5
	1.22–1.7			1.3–1.5	*2.09–2.36*	1.3–1.6
Y	*0.064*	2.67 **	–	0.19	*1.6*	3.1
	0.04–0.09	2–6		0.09–0.35	0.7–3.98	3.3–3.4

Determinations are performed at Institute of Geochemistry SB RAS (Irkutsk, Russia) with ICP-MS (by Sokolnikova Yu.V., Ponomareva V.Yu.) and AES (by Vasilyeva I.E.). A dash indicates that element was not determined

*Labeled the results were obtained for 35 samples, **labeled the results were obtained for 6 samples and ***labeled the results were obtained for 24 samples

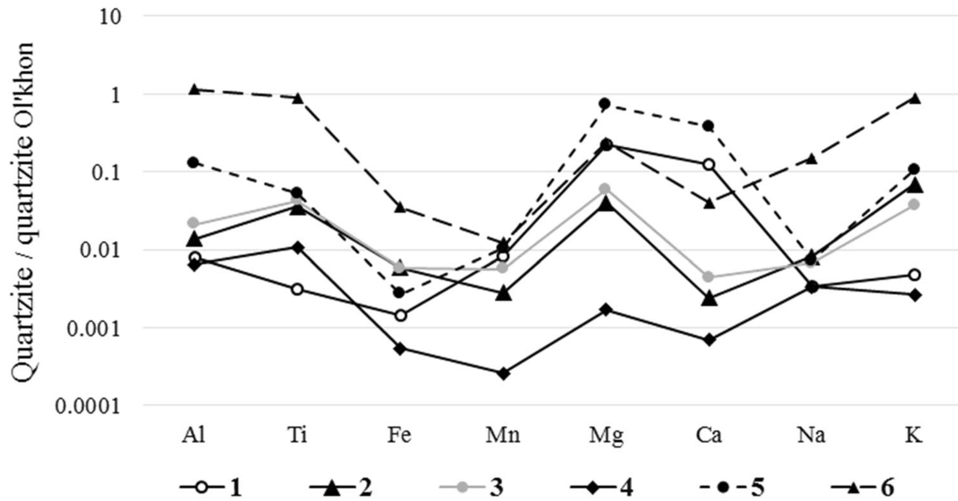

Fig. 7 Composition of quartzite varieties of the Irkut Formation normalized to average quartzite of the Olkhon area. 1. initial quartzite Urunge-Nur, 2. dark-grey quartzite of Bural-Sardyk, 3. white quartzite, 4. superquartzite of Bural-Sardyk, 5. initial quartzite of Urunge-Nur close to the contact with granitoids, 6. dark-grey quartzite near the contact with granitoids

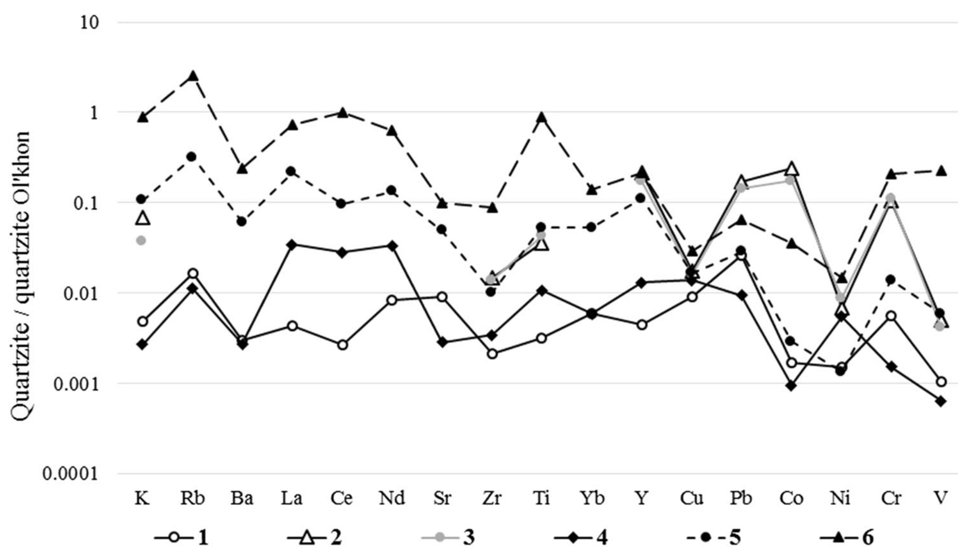

Fig. 8 Distribution of rare elements in quartzite varieties of Irkut Formation (East Sayan Mountains), normalized to average quartzite of Olkhon area. 1. initial quartzite of Urunge-Nur, 2. dark-grey quartzite of Bural-Sardyk, 3. white quartzite, 4. superquartzite of Bural-Sardyk, 5. initial quartzite of Urunge-Nur close to the contact with granitoids, 6. dark-grey quartzite near the contact with granitoids

In discolored light-grey and white quartzites, the total number of petrogenic elements relative to black quartzites from bedded bodies is about half, and in the purest superquartzites it is three times lower. There is no distinct correlation between the intensity of decoloration (color index) and the impurity amount. Thus, totally white discolored quartzites are not much different in the amount of impurities from light-grey ones, although the former are practically devoid of carbonaceous substance. At the same time, black and dark-grey bedded quartzites insignificantly yield to the discolored quartz varieties in the content of impurity elements.

The productive bedded sequence of quartzites at Bural-Sardyk is composed of relatively pure varieties of quartzites (about 400 ppm in black and dark-grey siliceous, 250 ppm in light-grey and grey, and about 100 ppm in superquartzites). The organic carbon content varies from 0.63 mass% (and more in dark-grey quartzites), to 0.36% in grey, and nearly total absence in superquartzites.

When comparing compositions of quartzites from cross-sections remote from granites and close to their contacts, it becomes evident that near-contact varieties are much enriched with granitephyle elements (Kozlov et al. 2008) (Tables 1, 2, Figs. 8, 9). This is undoubtedly related to the effect of granites. The light-grey and grey quartzites are marked by elevated (relative to superquartzites) Al, Fe, Ca, K, P, B, and Cr, and the contents of Rb, Cs, Ba, Nb, Y, and Hf are three times higher. Quartzites of the Irkut Formation experienced superposed processes of contamination in intrusive body contact zones of different generations and ages, resulting in a noticeable rise of petrogenic element contents, as well as rare granitephyle and rare-earth elements (REEs) (including Al, Ti, K, Y, and other REEs, as well as Ba, Rb, B, Cs). Additionally, there are increased contents of basic and ultrabasic elements, e.g. V, Ni, and

Table 3 Results on oxygen isotope composition in quartz samples from quartzites of Irkut Formation (East Sayan Mountains) (in ppm relative to SMOW)

N	Sample number	Rock	Location	d^{18}O ‰	Standard deviation (n)
1	229	Coarse-grained white quartzite (superquartzite)	Bural-Sardyk deposit, maximally altered by dynamic metamorphism	29.8	0.3 (2)
2	233	Coarse-grained white quartzite (superquartzite)	Bural-Sardyk deposit, maximally altered by dynamic metamorphism	29.8	0.0 (2)
3	176	Fine-grained grey quartzite	Bural-Sardyk deposit, altered by dynamic metamorphism	29.2	0.4 (3)
4	237	Fine-grained grey quartzite	Bural-Sardyk deposit, altered by dynamic metamorphism, contact with granitoids	26.3	0.1 (2)
5	822	Fine-grained dark-grey quartzite	Bural-Sardyk deposit, altered by dynamic metamorphism	29.7	0.1 (2)
6	238	Fine-grained dark-grey quartzite	Bural-Sardyk deposit, altered by dynamic metamorphism, contact with granitoids	27.1	0.0 (2)
7	239	Fine-grained dark-grey quartzite	Bural-Sardyk deposit, altered by dynamic metamorphism, contact with granitoids	26.5	0.0 (2)
8	302	Fine-grained grey quartzite	Urunge-Nur occurrence, poorly metamorphosed, at maximum distance from intrusive	29.3	0.2 (2)
9	295	Fine-grained grey quartzite	Urunge-Nur occurrence, poorly metamorphosed, contact with granitoids	27.1	0.1 (2)

Determinations are performed at Geological Institute SB RAS (Ulan-Ude, Russia)

Cr. This is possibly owing to the influence of ophiolite allochthons.

The quartzite sequence of the Irkut Formation is specifically marked by low contents of primarily Mn, Co, and Cu and enhanced Ca, Mg, and Fe due to the carbonate impurity.

The spidergram clearly shows contamination of quartzites near the contact with granites and purification of recrystallized quartzites both in petrogenic (Fig. 7) and rare elements (Fig. 8). In contrast to the petrogenic elements, the initial quartzites are impoverished in rare elements, whereas the near-contact varieties display enrichment in granitephyle elements, e.g. K, Rb, Ba, REEs, Sr, and Zr.

Superquartzites are characterized by particularly low impurities and carbonaceous material. These are not only the chemically purest variety of quartzite at Bural-Sardyk, but are also outstanding in purity within the entire quartzite family worldwide (Vorob'ev et al. 2003; Gotze 2012).

4.2.2 *Isotope-geochemical study of quartzite of East Sayan Mountains*

In magmatic, sedimentary and metamorphic rocks, the isotopic composition of oxygen varies broadly; a majority of silicate minerals are characterized by positive values of δ^{18}O lying within the range from +5‰ to +15‰ relative to SMOW.

Magmatic rocks show a tendency of increasing δ^{18}O with rising SiO_2 content from +5.4‰ to +6.6‰ in ultrabasic rocks to +7‰ to +13‰ in granitoids and pegmatites; in high-Si sedimentary rocks of quartz sandstone type, δ^{18}O values do not exceed +10‰, and in silica they may reach +35‰.

Values of δ^{18}O up to 42‰ are typical for recent organic marine sediments formed at low temperatures. Terrigenous sediments with silica have δ^{18}O values from 10‰ to 15‰ depending on the content of clastic and authigene material (Taylor 1974; Faure 1986).

Isotopic composition change of both intrusive and hosting rocks in the post-crystallization period is reported in Taylor (1974) and may extend beyond the contact metamorphism zone.

^{18}O content in quartzites may vary from 15‰ to 35‰ (Savin and Epstein 1970; Karhu and Epstein 1986; Knaut and Epstein 1986; Sharp et al. 2002). However, ^{18}O contents in quartzite on all continents of the Earth in the Neo-Proterozoic period are constrained from 20‰ to 30‰ (Bindeman et al. 2016).

Available results on the isotopic composition of oxygen of quartzites in the East Sayan Mountains show maximum values for both initial poorly metamorphosed (sample 302) and all types of rocks of bedded cross-section (superquartzite samples 229, 233; 176, fine-grained grey; and 822, fine-grained dark-grey) (Table 3). In the zone of contact influence of granitoids on both sites, the ^{18}O isotopic composition in quartzite shifts towards low values.

Some sites of bedded bodies were affected by granitoids, as indicated by the isotope composition change (sample 237, fine-grained grey). They were, however, recrystallized with evacuation of carbonaceous substance.

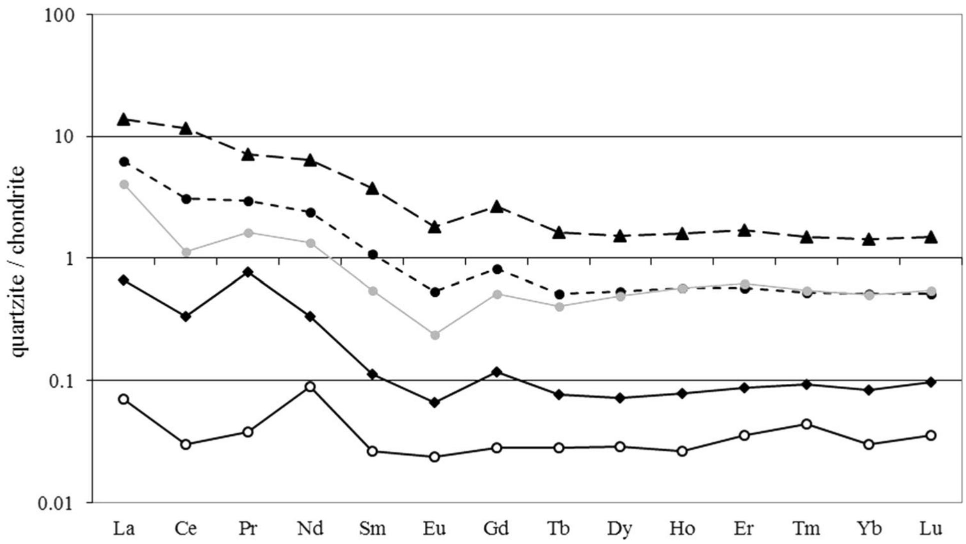

Fig. 9 Distribution of rare-earth elements in quartzite varieties of Irkut Formation (East Sayan Mountains), normalized to chondrite (Evensen et al. 1978). 1. initial quartzite of Urunge-Nur, 2. dark-grey quartzite of Bural-Sardyk, 3. white quartzite, 4. superquartzite of Bural-Sardyk, 5. initial quartzite of Urunge-Nur close to the contact with granitoids, 6. dark-grey quartzite near the contact with granitoids

5 Discussion of results and model of superquartzite formation

The models proposed before could not fully account for the geologic setting and processes of productive quartzite purification at the Bural-Sardyk deposit and other locations. They do not provide a clear justification for the recently proposed patterns including:

- Morphology of productive bodies at Bural-Sardyk and other occurrences not involved in this work dip gently in northwestern and northern directions and do not coincide with the steeply dipping siliceous-carbonate sequence of the Irkut Formation. The azimuths of dipping of beds and lenses of superquartzites and discolored quartzites are oriented across strike of overthrust units occurring in the frontal part.
- Geochemical zonation with discoloration and depletion in element impurities is observed from bottom to top, so that maximally processed superquartzites and discolored quartzites lie at the top of the cross-section. In the same direction, the increased size of quartz grains and subparallel orientation of porphyry-like elongated quartz inclusions indicates thermal-dynamic impact.
- The position of bedded and lens-like bodies of superquartzites and discolored quartzites is not controlled by granitoids. Considering the content of impurity elements, the quartzites are subdivided into superquartzites, light-grey, and black bedded at Bural-Sardyk; and near-contact and initial quartzites at Urunge-Nur. REE content increases from initial quartzites to near-contact ones at Urunge-Nur site, and from superquartzites to black near-contact ones at Bural-Sardyk. The superquartzites occupy an intermediate position between initial and near-contact quartzites. Furthermore, the initial quartzites do not show europium, while it does appear in superquartzites and intensifies in near-contact quartzites of Bural-Sardyk.

Considering Paleo–Asian Ocean evolution, and petrographic and geochemical features of the metamorphic-sedimentary siliceous-carbonate sequence discussed in this work, we infer a complex multi-phase process of its transformation resulting in formation of unique superquartzites.

The sedimentary sequence of siliceous rocks of the Gargan Block derived through deposition of the basal bedded sequence of limestones aged 1.25 Ga (Kuznetsov et al. 2010) after insignificant marine transgression (Semeikin et al. 2006; Il'in 2009). The siliceous sequence accumulated under transitional zone conditions from extensive shelf to continental slope as a result of upwelling of deep waters (Degens 1965) and chemogenous deposition of silica, as indicated by high isotopic tags of oxygen ($d^{18}O > 29.2$‰, Table 3). The sedimentary-marine origin is indicated by low Ce in initial quartzites of the Urunge-Nur site retained in metamorphosed quartzites of the Bural-Sardyk deposit (Fig. 9). If coastal sands were the exclusive source rocks for these quartzites, the quartz composition would be much more complex, as previously reported (Armstrong-Altrin et al. 2012, 2014, 2015a, b, 2017). Additionally, a fairly poor impurity of terrigenous component in rocks is confirmed by low contents of impurity elements in nearly all source quartzites and in ore bodies. During the entire period of sedimentary sequence formation, the sea experienced numerous small-amplitude cycles of transgression and regression that are reflected in rhythmic intercalation of silica beds with carbonate seams (Semeikin et al. 2006). Such tectonic activity proceeded through a time span sufficient for forming 1 km (on

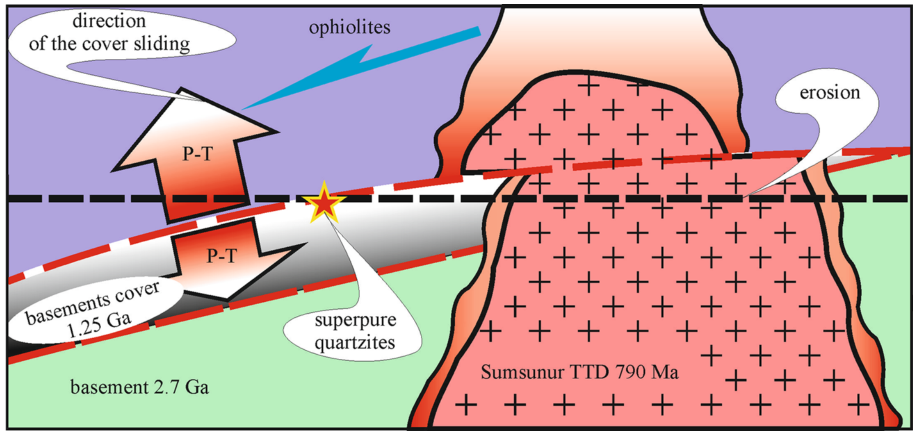

Fig. 10 Schematic of gravitational sliding of ophiolite cover over the Gargan Block cover and dynamothermal effect on the sediments of the block

average) of siliceous-carbonate sequence sediments (Fig. 1). Later on, the sea regressed, and the rocks of the Irkut Formation were overlapped by terrigenous, volcanic-sedimentary material of the Urtagol Formation.

At the same epoch, the Dunzhugur island arc formed WNW off the Gargan Block, and started to move toward the continental margin (Kuzmichev 2004; Zhmodik et al. 2006). At the stage of marginal sea shrinkage, the existing subduction zone inclined beneath the island arc. After the island arc had joined the continent, the subduction zone moved underneath the Gargan Block, and supra-subduction granitoids of the Sumsunur complex melted (Kuzmichev et al. 2001; Kuzmichev 2004). The Sumsunur complex intrusions broke through the basement of the Gargan Block, and through its silica-carbonate and ophiolite cover. In the near-contact zone they intensely contaminated fairly clean beds of quartzites of the Gargan Block cover. Alteration of host rocks resulted in elevated contents of sericite, and major and trace elements uncommon for these rocks in the near-contact quartzites (Figs. 8, 9).

Granitization of rocks and melting of the Sumsunur granitoids brought about isostatic buoyancy of the Gargan Block with overlapping ophiolites and subsequent sliding of tectonic nappe over the silica-carbonate cover, stripping the upper schistose and carbonate parts and affecting the siliceous bedded sequence (Fig. 10) in the northwest and southeast. Due to sliding from the emerging block, the ophiolite cover heaped and crumpled in its environment and acquired scale-like shape.

Pressure–temperature (P–T) conditions in the sliding slab bottom measured specifically for Bural-Sardyk superquartzites as 400–410 °C and 2.5 kb (Krylova et al. 2004) lead to recrystallization and mobilization of the fluid component of initial siliceous rocks and its migration through faults and weak zones into a low-P field. It is apparent that most impurities moved into the uppermost sites due to isostatic pressure drop. However, some impurities migrated from top to bottom. Segments of siliceous sequence occurring at horizons remote from the tectonic contact with relatively low P–T conditions experienced smaller impact. Therefore, they also underwent reduced recrystallization, and could become the area of discharge for impurity-elements from the above-lying sequences. Such a zone of discharge for migrating elements and coaly substance is—in our view—the horizon of black quartz-sericite schists with talc, graphite, and manganocummingtonite about 1–2 m thick at the bottom of the quartzite bedded sequence of the Irkut Formation. Such P–T conditions are common for different geodynamic settings, including the ophiolite cover bottom (Peacock 1987). They are referenced as the structures of inverted metamorphic zonation in overthrust (Ghent and Stout 1981; Donskaya et al. 2004) and subduction zones (Duebendorfer 1988). Some authors note presence of thin (some meters) relatively high-T zones at the bottom of ultrabasic rocks replaced by low-T zones downsection, their thickness varying from tens to hundreds of meters.

Sliding of the allochthon at the top of the quartzite cross-section under maximum uni-directional discrete-dynamic effect caused recrystallization of initial quartz substratum with increasing quartz grain size and formation of specific texture (Figs. 3, 4a–4b, 5) of superquartzites (Grigoriev 1956). It reflects the cover movement direction by principles previously described (Vernon 1980; Tripathy et al. 2009; Popov 2011). Low P–T sites of siliceous sequence occurring at horizons remote from the tectonic contact experienced a smaller effect. Therefore, they have undergone a lower degree of recrystallization, and could become the discharge area for impurity elements from overlying sequences. Reduction of the transformation degree of quartzites farther from the plane of tectonic contact, with the increase of impurity contents being characteristic of the quartzite proper, is evidence of the presence of a fluid component from the rocks proper and of the absence of endogenous fluid inflow. It should be noted that quartzites were discolored due to entire or partial removal of pigmenting carbonaceous substance.

The quartzite textures above have been described in polymineral rocks, such as Emizözü granitoids (Turkey) deformed in shear zones (Isik 2009). An analogous geochemical pattern was reported in (Polat et al. 1996), who observed an increase of SiO2, Zr, Th, Hf, and LREEs; and of LREE/HREE, LREE/Sc, Th/Sc ratios from top to bottom, as well as a decrease of TiO_2, MgO, V, Co, Ni, and Sc in sandstones, quartzites, and shales of tectonic mélange.

In recrystallization and decontamination from REE impurities with formation of superquartzites, the rocks retain distinct Eu depletion, and total content of light lanthanoids is increased (Fig. 9). Such behavior of rare-earth and other elements, as well as lightening of oxygen isotopic composition in quartz of quartzites—to 26.3‰–27.1‰ at Bural-Sardyk and to 27.1‰ at Urunge-Nur—indicates that in the history of quartzite transformation at these deposits, it is feasible to recognize the stage of their contamination linked with intrusion.

Dynamometamorphic transformations of silicites into "superquartzites" and other types of quartzites occurred in collapse, rather than in the underwater regime, as a result of the emergence of the Gargan Block and subsequent gravitational landslide of ophiolite complex rocks. The evidence for this includes azimuths of incidence of stratal bodies and glide mirrors of the studied areas directed toward the northwest on the western block slope and the southeast on its eastern slopes. In this case, there is a natural relationship between the azimuths of the fall of quartzite bodies and the azimuths of the strike of discontinuous structures of different rank developed in the frontal sector. If recrystallization occurred during the development of ophiolite obduction, the orientation of the azimuths of the fall of productive bodies would be close to one direction and not controlled by a system of tectonic structures.

The proposed model of formation of superquartzites and other types of quartz dynamomorphites or dynamometasomatites at the western slope of the Gargan Block is simplified without considering variations of event history. It is targeted to disclose the mechanism itself and principal conditions of quartzite recrystallization that result in superquartzite formation.

6 Conclusions

The unique deposit of super pure quartzites referred to as the Bural-Sardyk type could have formed by ongoing geologic and tectonic processes and events in combination. Comprehensive petrographic and geochemical studies revealed some evidence suitable to derive some inferences on this issue.

(1) Highly sensitive analytical methods identified truly unique chemical purity of original micro- and ultramicro-quarzites of the Bural-Sardyk deposit. Low content of impurity elements (hundreds of ppm) in the source microquarzites along with insignificant variations in carbonate content point to their formation over the lower boundary of carbonate rock sedimentation, i.e. at the top of the continental slope. In this case, the geodynamic setting of sedimentation is reconstructed as the deep fore-arc basin with the chemical sedimentation of siliceous material.

(2) Sediments are overlapped by a thick layer of allochthonous rocks through accretion of the block cover and ophiolite obduction.

(3) Tectonic uplift of the basement as a result of granitization of the crustal block and intrusion of plagiogranites triggered the Gargan Block rising, preceding subhorizontal tectonic movement. Intrusions of supra-subduction granitoids were responsible for contamination of near-contact quartzites with granitephyle elements and for changes to the isotopic composition of rocks.

(4) Sliding of the block cover uncompensated by erosion, with its dynamothermal reworking of the bed, actively involved serpentine slabs of ophiolite cover with talc at their base. Their movement carried away the underlying sedimentary cover, causing slight warming and recrystallization of quartzites accompanied by decolorization and decontamination of impurities from near-contact and remote rocks. The dynamic mechanism is verified by structures oriented toward the movement of reworked overlying superquartzites, reduction of dynamometamorphic alteration at depth, and numerous slickensides within the Irkut Formation rocks transferred from the Gargan Block center.

(5) The mechanism of purifying quartz derived from quartzites of the Bural-Sardyk deposit due to tectonic sliding of overlying rocks is not unique and may be confirmed by other quartz deposits.

Acknowledgements The work was performed under financial support of Integration Program No. 0341-2016-001 and Russian Foundation for Basic Research Projects 15-05-02772a and 18-05-00439a with research equipment isotope-geochemical studies at IGC SB RAS. We appreciate constructive comments from Skuzovatov S. Yu that significantly improved the quality of the paper. The authors thank sincerely Tatiana Bunaeva for preparation of the English version of the text.

References

Anfilogov VN, Kabanova LY, Igumentseva MA, Nikandrova NK, Lebedev AS (2015) Geological structure, petrography and mineralogy of the quartzite depozite Bural-Sardag. Prospect Prot Mineral Resour 7:19–23 **(in Russian)**

Anisimova IV, Levitsky IV, Kotov AB et al (2009) Age of the Gargan Block basement in the East Sayan Mts: results on U-Pb geochronology research. In: Proceedings IV Russian Conference Isotope Geochronology, St. Petersburg, IPGG RAS:35-36

Armstrong-Altrin JS (2015) Evaluation of two multi-dimensional discrimination diagrams from beach and deep sea sediments from the Gulf of Mexico and their application to Precambrian clastic sedimentary rocks. Int Geol Rev 57(11–12):1446–1461

Armstrong-Altrin JS, Lee YI, Kasper-Zubillaga JJ, Carranza-Edwards A, Garcia D, Eby N, Balaram V, Cruz-Ortiz NL (2012) Geochemistry of beach sands along the western Gulf of Mexico, Mexico: implication for provenance. Chemie der Erde/Geochemistry 72:345–362

Armstrong-Altrin JS, Nagarajan R, Lee YI, Kasper-Zubillaga JJ, Córdoba-Saldaña LP (2014) Geochemistry of sands along the San Nicolás and San Carlos beaches, Gulf of California, Mexico: implications for provenance and tectonic setting. Turk J Earth Sci 23(5):533–558

Armstrong-Altrin JS, Machain-Castillo ML, Rosales-Hoz L, Carranza-Edwards A, Sanchez-Cabeza JA, Ruíz-Fernández AC (2015) Provenance and depositional history of continental slope sediments in the Southwestern Gulf of Mexico unraveled by geochemical analysis. Cont Shelf Res 95:15–26

Armstrong-Altrin JS, Lee YI, Kasper-Zubillaga JJ, Trejo-Ramírez E (2017) Mineralogy and geochemistry of sands along the Manzanillo and El Carrizal beach areas, southern Mexico: implications for palaeoweathering, provenance, and tectonic setting. Geol J 52(4):559–582

Belichenko VG, Reznitsky LZ, Geletii NK, Barash IG (2003) Tuva-Mongolian terrane (in the context of microcontinents in the Paleoasian Ocean). Russ Geol Geophys 44(6):554–565

Bindeman IN, Bekker A, Zakharov DO (2016) Oxygen isotope perspective on crustal evolution on early Earth: a record of Precambrian shales with emphasis on Paleoproterozoic glaciations and Great Oxygenation Event. Earth Planet Sci Lett 437:101–113

Bydtaeva NG, Kiseleva RA, Mileeva IM (2006a) Preliminary assessment of the quality of quartz with the purpose of forecasting its technological indicators. The results of fundamental and applied research. Karelian Research Centre, Petrozavodsk, pp 112–119

Bydtaeva NG, Kiseleva RA, Mileeva IM (2006b) Forecast-search model of deposits of high purity quartz. Natl Geol 4:57–63

Danilevskaya LA, Schiptsov VV (2007) Status and resources of the mineral resource base of the Republic of Karelia. Prospect Prot Mineral Resour 10:29–33

Danilevskaya LA, Skamnitskaya LS, Schiptsov VV (2004) Silica raw materials of Karelia. Karelian Research Centre of Russian Academy of Sciences, Petrozavodsk

Degens ET (1965) Geochemistry of sediments. A brief survey. Prentice-Hall, Inc., Englewood Cliffs, NJ

Demonterova EI, Ivanov AV, Reznitskii LZ, Belichenko VG, Hung C-H, Chung S-L, Yo Iizuka, Wang K-L (2011) Formation history of the Tuva-Mongolian massif (Western Hubsugul region, North Mongolia) based on U–Pb dating of detrital zircons from sandstone of the darkhat group by the LA-ICP-MS method. Dokl Earth Sci 441(1):1498–1501

Dobretsov NL (1985) On nappe 'tectonics' of East Sayan. Geotectonics 1:39–50

Donskaya TV, Sklyarov EV, Gladkochub DP, Mazukabzov AM, Vasil'ev EP (2004) The Shutkhulai metamorphic complex, Southeastern Sayans: specific features of metamorphism and a model of formation. Russ Geol Geophys 45(2):194–211

Duebendorfer EM (1988) Evidence for an inverted metamorphic gradient associated with a Precambrian suture, southern Wyoming. J Metamorph Geol 6(1):41–63

Evensen NM, Hamilton PJ, O'Nions RK (1978) Rare-earth abundances in chondritic meteorites. Geochim Cosmochim Acta 42(8):1199–1212

Faure G (1986) Principles of isotope geology, 2nd edn. Wiley, New York

Fedorov AM, Makrygina VA, Budyak AE, Nepomnyashchikh AI (2012) New data on geochemistry and mechanism of formation of quartzites of the Bural-Sardyk deposit (Eastern Sayan Mts). Dokl Earth Sci 442(1):120–125

Ghent ED, Stout MZ (1981) Metamorphism at the base of the Samail Ophiolite, Southeastern Oman Mountains. J Geophys Res 86(NB4):2557–2571

Gordienko IV (2006) Geodynamic evolution of late Baikalides and Paleozoides on the folded periphery of the Siberian Craton. Russ Geol Geophys 47(1):53–70

Gotze J (2012) Classification, mineralogy and industrial potential of SiO_2 minerals and rocks. In: Gotze J, Mockel R (eds) Quartz: deposits, mineralogy and analytics. Springer, Heidelberg, pp 1–28

Grebenshchikova VI, Koval PV (2004) Geochemistry of tonalite formation in the Sumsunur batholith, Eastern Sayan. Petrology 12(1):56–69

Grigoriev DP (1956) The recrystallisation of minerals. Zap Sov Mineral Soci 85(2):147–170

Il'in AV (2009) Neoproterozoic ferriferous quartzites. Lithol Miner Res 1:87–95

Isik V (2009) The ductile shear zone in granitoid of the Central Anatolian Crystalline Complex, Turkey: implications for the origins of the Tuzgölü basin during the Late Cretaceous extensional deformation. J Asian Earth Sci 34(4):507–521

Jung L (1992) High purity natural quartz. Part I: high purity natural quartz for industrial use. Quartz Technology, Liberty Corner, New Jersey

Kabanova LY, Anfilogov VN, Nepomnyaschih AI, Igumentzeva MA (2014) Petrographic features of quartzites from Bural Sar′dak (East Sayan Mountains). Lithosphere 1:81–94

Karhu J, Epstein S (1986) Hidrogen and oxygen isotope ratios in nodular and bedded cherts. Geochim Cosmochim Acta 40:1095–1108

Knaut LP, Epstein S (1986) The implication of the oxygen isotope record in coexisting cherts and phosphates. Geochim Cosmochim Acta 50:1745–1756

Kozlov VD, Spiridonov AM, Chokan VM (2008) Petrological-geochemical features and metallogenic specilaization of the granitoids of the Lubava-khapcheranga ore district, Central Transbaikalia. Izv Sib Otd-niya Sektsii Nauk O Zemle RAEN Geologiya, Poiski i Razvedka Rudnykh Mestorozhdenii 7(33):4–17

Krylova GI, Skobel LS, Mitrofanov AA, Balakirev VG (2003) Geological and mineral-geochemical data of quartz having brand IOTA, USA, South Carolina scope for searching its analogues in Russia. Ural Geol J 4(34):81–122

Krylova GI, Kreisberg VA, Mitrofanov AA, Astafjevs VN (2004) Gas saturation of quartz materials and gross water content. In: Materials of the XI international conference on thermobarogeochemistry. Aleksandrov, pp 320–354

Kuzmichev AB (2001) Early Baikalian tectonic events in the Tuva-Mongolia Massif. Geotectonics 35(3):185–198

Kuzmichev AB (2004) The tectonic history of the Tuva–Mongolia massif: Early Baikalian, Late Baikalian and Early Caledonian Stages. Probel-2000, Moscow

Kuzmichev AB, Bibikova EV, Zhuravlev DZ (2001) Neoproterozoic ($\sim$ 800 Ma) orogeny in the Tuva-Mongolia Massif (Siberia): island arc–continent collision at the northeast Rodinia margin. Precambr Res 110(1–4):109–126

Kuznetsov SK, Lutoev VP, Kotova EN, Chuprov GV, Shanin SN (2005) The problem of high-purity quartz raw materials of Russia. Vestn Inst Geol Komi Sci Center Ural Branch RAS 5:5–9

Kuznetsov AB, Konstantinova GV, Kutyavin EP, Letnikova EF, Vishnevskaya IA, Geletii NK (2010) Sr-chemostratigraphy of carbonate sedimentary cover of the Tuva-Mongolian microcontinent. Dokl Earth Sci 432(1):577–582

Makrygina VA, Fedorov AM (2013) Quartzite transformation as a consequence of late tectonic events in the evolution of the Chuya and Gargan blocks. Russ Geol Geophys 54(12):1450–1457

Muller A, Ihlen PM, Wanvik JE, Flem B (2007) High-purity quartz mineralization in kainite quartzites, Norwey. Miner Depos 42:523–535

Nepomnyashchikh AI, Krasin BA, Vasilieva IE, Yeliseyev IA, Eremin VP, Fedosenko VA, Sinitskii VV (2000) Silicon for solar energy. Bull. Tomsk Polytech Univ 303(2):176–190

Nepomnyashchikh AI, Demina TV, Zhaboedov AP, Eliseev IA, Lesnikov PA, Lesnikov AK, Paklin AS, Romanov VS, Sapozhnikov AN, Sokol'nikova YuV, Fedorov AM, Shalaev AA, Shendrik RYu (2017) Optical silica glass based on super quartzites from the Eastern Sayan Mountains. Glass Phys Chem 43(3):222–226

Peacock SM (1987) Creation and preservation of subduction-related inverted metamorphic gradient. J Geophys Res 92(B12):12763–12781

Petrova ZI, Koneva AA, Makrygina VA (1996) Geochemistry of quartzites and quartzitoschists of the Olhon region (Western Baikal area). Geochem Int 33(9):109–127

Polat A, Casey JF, Kerrich R (1996) Geochemical characteristics of accreted material beneath the Pozanti-Karsanti ophiolite, Turkey: intra-oceanic detachment, assembly and obduction. Tectonophysics 263(1–4):249–276

Popov VA (2011) Crystallization and recrystallization in quartz bodies. In: Materials of conference "Modern problems of studying and use of the mineral resource base of quartz—2011". Miass-Ekaterinburg, pp 142–145

Reznitsky LZ, Barash IG, Belichenko VG, Kotov AB, Sal'nikova EB, Glebovitsky VA, Kovach VP, Yakovleva SZ, Fedoseenko AM (2007) Upper age boundary of the accretion of terranes in the northwestern part of the Eastern segment of the Central Asian foldbelt. Dokl Earth Sci 414(4):548–551

Safonova IYu, Santosh M (2014) Accretionary complexes in the Asia-Pacific region: tracing archives of ocean plate stratigraphy and tracking mantle plumes. Gondwana Res 25(1):126–158

Savin SM, Epstein S (1970) The oxygen and hydrogen isotope geochemistry of ocean sediments and shales. Geochim Cosmochim Acta 34:43–63

Semeikin IN, Dolnik TA, Titorenko TN (2006) Cyclic stratigraphy and ore capacity of Riphean-Paleozoic sediments of Oka-Kitoy area (East Sayan). Izv Sib Dept Earth Sci Sect 3(29):84–104

Serykh NM, Borisov LA, Gulin EN, Caireac AD (2003) On the prospects of quartz use in the Russian mineral resource base for high technology industry. Prospect Prot Miner Resour 1:17–20

Sharp ZD, Durakiewicz T, Migaszewski ZM, Atudorei VN (2002) Antiphase hidrogen and oxygen isotope periodicity in chert nodules. Geochim Cosmochim Acta 66:2865–2873

Sklyarov EuV, Dobretsov NL (1987) Metamorphism of ancient ophiolites of east and West Sayan. Russ Geol Geophys 28:43–54

Taylor HP (1974) The application of oxygen and hydrogen isotope studies to problems of hydrothermal alteration and ore deposition. Econ Geol 69:843–883

Tripathy NR, Srivastava HB, Mamtani MA (2009) Evaluation of a regional strain gradient in mylonitic quartzites from the footwall of the Main Central Thrust Zone (Garhwal Himalaya, India): inferences from finite strain and AMS analyses. J Asian Earth Sci 34(1):26–37

Tsarev DI, Khrustalev VK, Ayurzhanaeva DT, Galchenko VI (2007) Geology and genesis of the Cheremshanka silica deposit, Western Transbaikal region. Russia. Geology of Ore Deposits 49(4):297–307

Vernon RH (1980) Metamoprhic processes. Reactions and development of microstructure. Transl. Engl., Moscow: Nedra, Publ. H., Great Britain, 1976

Volkova MG, Nepomnyashchikh AI, Fedorov AM, Makhlyanova AM, Bryanskii NV (2017) Fluid inclusions in "superquartzites" of the Bural-Sardyk deposit (East Sayan). Russ Geol Geophis 58(9):1053–1058

Vorob'ev EI, Spiridonov AM, Nepomnyashchikh AI, Kuz'min MI (2003) Superpure quartzites of the Eastern Sayan (Burayt Republic, Russia). Dokl Earth Sci 390(4):497–500

Zhmodik SM, Postnikov AA, Buslov MM, Mironov AG (2006) Geodynamics of Sayan-Baikal-Muya accretion-collision belt in Neoproterozoic-Early Paleozoic, pattern of formation and localization of noble metal mineralization. Russ Geol Geophys 47(1):183–197

Zorin YuA, Sklyarov EV, Belichenko VG, Mazukabzov AM (2009) Island arc-back-arc basin evolution: implications for late Riphean-Erly Paleozoic geodynamic history of the Sayan-Baikal folded area. Russ Geol Geophys 50(3):149–161